THE DIFFERENTIATION OF MUSCLE CONTAINING MYOFASCIAL TRIGGER POINTS FROM HEALTHY MUSCLE USING ULTRASOUND

by

Matthew D. Bird

A Thesis
Submitted to the
Graduate Faculty
of
George Mason University
In Partial Fulfillment of
The Requirements for the Degree
of
Master of Science
Bioengineering

Committee:

_____	Dr. Parag Chitnis, Thesis Director
_____	Dr. Siddhartha Sikdar, Committee Member
_____	Dr. Lynn Gerber, Committee Member
_____	Dr. Michael Buschmann, Chairman, Department of Bioengineering
_____	Dr. Kenneth S. Ball, Dean, Volgenau School of Engineering

Date: _____ Spring Semester 2019
George Mason University
Fairfax, VA

The Differentiation of Muscle Containing Myofascial Trigger Points from Healthy Muscle Using Shear Wave Elastography

A thesis submitted in partial fulfillment of the requirements for the degree of Master of Science at George Mason University

By

Matthew D. Bird
Bachelor of Science
George Mason University, 2016

Director: Dr. Parag Chitnis, Professor
Department of Bioengineering

Spring Semester 2019
George Mason University
Fairfax, VA

Dedication

I dedicate this thesis to my family: my mother and father, my sister Alison, and my stepmother Ye-Ling. Without their constant love, support, and belief in me, I would not have made it so far. Everything I have accomplished I owe to them.

Acknowledgments

The completion of the work within this thesis would not have been possible without the support of my advisors and mentors, Dr. Siddhartha Sikdar, Dr. Parag Chitnis, and Dr. Lynn Gerber. I would like to thank them for sharing their valuable time and insightful advice with me and for always keeping my best interests in mind. I would also like to thank my collaborators Dr. Jay Shah, Secili DeStefano, Hannah Tandon, and Vy Phan for their contributions to this project. Their assistance and feedback made subject data collections a day I would look forward to all week. Lastly, I would like to thank my colleagues, coworkers, and most importantly my friends, Dr. Biswarup Mukherjee, Dr. Amir Khan, Dr. Paul Otto, Dr. Nima Akhlaghi, Shriniwas Patwardhan, Ahmed Bashatah, Joseph Majdi, Ananya Dhawan, Giovanni Giammanco, April Aralar, and David Le. They made every day in lab a more fulfilling and enjoyable experience.

Table of Contents

List of Tables

List of Figures

Abstract

THE DIFFERENTIATION OF MUSCLE CONTAINING MYOFASCIAL TRIGGER POINTS FROM HEALTHY MUSCLE USING SHEAR WAVE ELASTOGRAPHY

Matthew D. Bird

George Mason University, 2019

Thesis Director: Dr. Parag Chitnis

Myofascial trigger points (MTrPs) are palpable, painful nodules that develop in skeletal muscle and are a characteristic finding in myofascial pain syndrome (MPS), a common chronic pain condition. Symptomatic MTrPs are frequently the target of therapeutic treatment for the management of MPS. However, the pathophysiology of MTrPs is poorly understood and the diagnostic criteria remain inconsistent. Based on previous investigations into MTrPs using ultrasound imaging, we hypothesized that muscles containing MTrPs have heterogeneous fiber orientation within the affected zone and surrounding areas compared to palpably normal muscle. For this study, we sought to utilize the known variation of shear wave speed with muscle fiber orientation as a method of determining anisotropy in muscle fibers. We developed a standardized method of acquiring shear wave elastography images at different transducer orientations using a custom transducer holder with a fixed imaging window. The holder was fitted over palpable MTrPs in the upper trapezius of patients suffering from chronic neck pain (>3 months). The transducer holder allowed for registration of the palpable MTrPs to any collected images. The variation of the shear wave speed of the muscle, as a function of the transducer angle, was used as a surrogate for muscle fiber orientation. The asymmetry of the fiber orientation was then determined and compared

between active (spontaneously painful) MTrPs, latent (not spontaneously painful) MTrPs, and normal muscle tissue. The results of this study showed an increase in muscle fiber asymmetry with increasingly symptomatic muscle, with normal muscle having the lowest asymmetry (6.64 ± 7.23 °, N = 11), then latent MTrPs (11.51 ± 9.86 °, N = 22), and finally active MTrPs (14.19 ± 11.76 °, N = 40). A statistically significant difference was found between the normal and active MTrPs groups ($p<0.014$). This data suggests that disruption of muscle fiber architecture may be an important feature that distinguished active MTrPs from normal muscle tissue.

Chapter 1: Introduction

Chronic pain is a poorly understood yet widespread and continuously growing problem [1]. Chronic pain affects approximately 20% of adults in developed countries. In the United States as many as 100 million adults suffer from chronic pain with an associated economic cost of $560-635 billion annually [1, 2]. Despite its widespread prevalence and increasing awareness, chronic pain remains under-diagnosed and under-treated [1]. When treatment for chronic pain is sought, it can often be misunderstood, misdiagnosed, and/or simply medicated by physicians [3]. Chronic pain is a condition that becomes more common as we age [1, 4]. As life expectancy continues to increase worldwide [5], and with a growing elderly population, it is becoming more important than ever to deepen our understanding of chronic pain.

Myofascial pain syndrome is the most common cause of chronic pain, usually affecting the neck or lower back [6–8]. Myofascial pain syndrome affects approximately 30% of primary care clinic patients and 85-93% of patients in specialty pain centers [9]. A characteristic finding in myofascial pain syndrome is the development of myofascial trigger points. Trigger points are defined as tender, taut, palpable nodules that form in the skeletal muscle [8]. Trigger points come in two varieties: active trigger points which cause spontaneous pain, and latent trigger points which only cause pain upon palpation [10, 11]. The role of trigger points in myofascial pain syndrome is currently not well understood. This is due to a lack of understanding of the soft tissue neighborhood of the muscles involved.

The purpose of this study was to further the understanding of how the presence of trigger points affects the local musculature. I propose the use of shear wave elastography ultrasound in order to measure differences between subjects suffering from myofascial pain syndrome associated with trigger points and those with no pain. Ultrasound provides a

relatively inexpensive, safe, and noninvasive method for the examination of the skeletal muscle, while the use of shear wave elastography allows for a quantitative measurement to be taken and correlated to the subject's pain level. This could be used to create a metric to evaluate the success of clinical intervention for myofascial pain syndrome.

Chapter 2: Background

2.1 Muscle Physiology

The human body contains three different types of muscle: skeletal, cardiac, and smooth. Of these, only skeletal muscle is responsible for voluntary contraction, while also helping to maintain and protect the skeletal system.

Skeletal muscle is wrapped in a sheath of dense, irregular connective tissue called epimysium, allowing for contraction while maintaining its structural integrity. Each muscle contains bundles of fibers called fascicles held together with a connective tissue called perimysium. Each fascicle bundle contains a connective tissue called the endomysium that encapsulates between 10-100 muscle fibers. These muscle fibers are the cells that make up the muscle and are some of the longest in the human body, with lengths up to 30cm. The muscle fibers can be further broken down into a cluster of myofibrils within a plasma membrane called a sarcolemma, demonstrated by Figure 2.1.

The contractile element of the muscle is the sarcomere, show in Figure 2.2, a highly organized arrangement of actin and myosin proteins that comprise the myofibril. The sarcomere is a repeating unit throughout the myofibril with the boundary between sarcomere units called the Z-line. Contraction begins at the motor end-plate when a motor neuron releases the neurotransmitter acetylcholine (ACh) into the synaptic cleft. The ACh binds to receptors in the sarcolemma causing the depolarization of the muscle fiber triggering an action potential. The action potential depolarizes the membrane, forcing the release of calcium ions and allowing the uptake of sodium ions. The calcium ions initiate the contraction which is then sustained with adenosine triphosphate (ATP); an organic molecule that is the primary source of energy throughout the body. While calcium ions remain in the sarcoplasm, and there is available ATP, muscle fibers will continue shortening through

a process known as the sliding filament model.

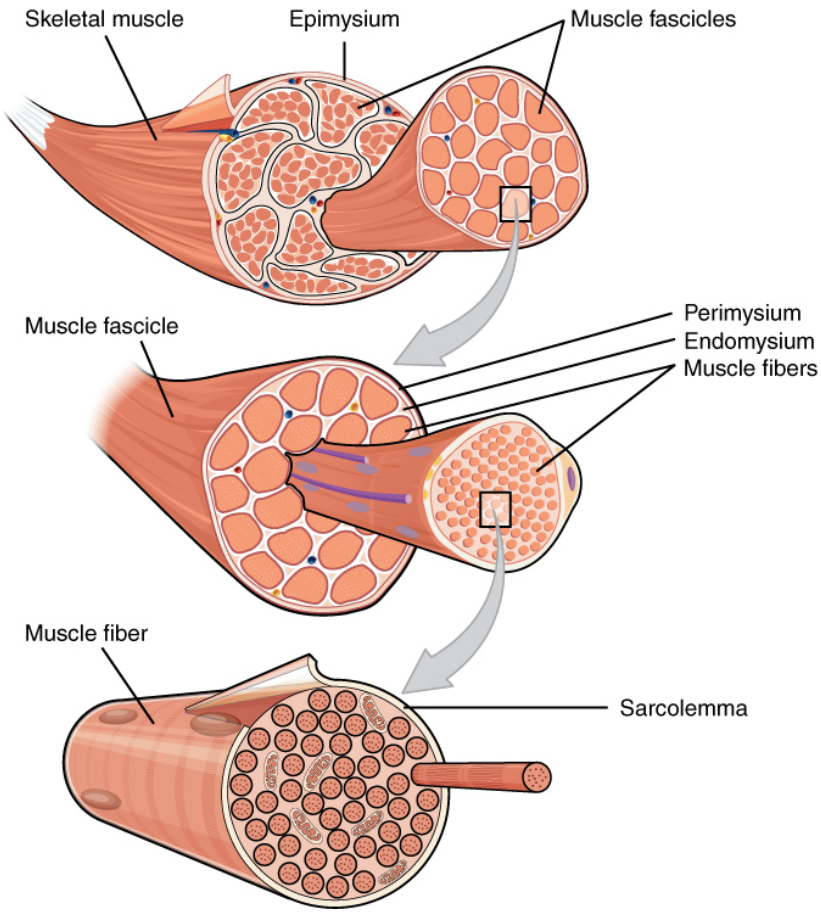

Figure 2.1: The anatomy of skeletal muscle [12].

The sliding filament model describes how the actin and myosin protein components of the sarcomere slide past each other when signaled to contract, as demonstrated in Figure 2.3. This is caused when myosin-binding sites on the actin filaments are revealed by the calcium ions within the sarcoplasm. This begins the cross-bridge cycle in which the myosin is able to bind to actin and slightly pull it before releasing. While ATP is present, the myosin will continue to re-attach and pull the actin further until the muscle is fully contracted. Notably, the region between the Z-lines decreases but all components remain the same length.

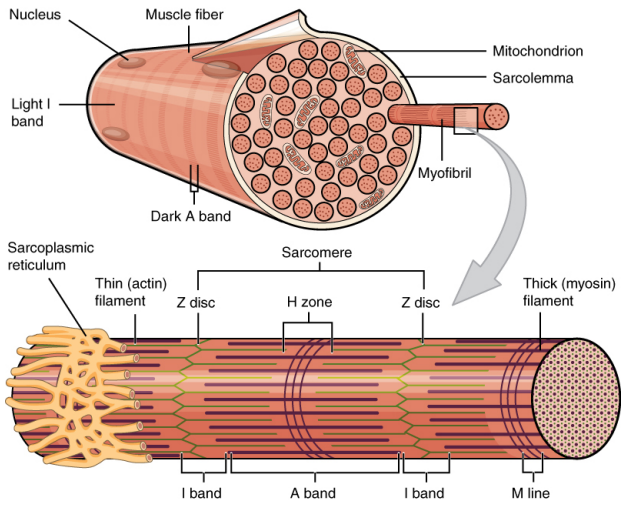

Figure 2.2: The anatomy of the muscle fiber and the myofibrils contained within it [12].

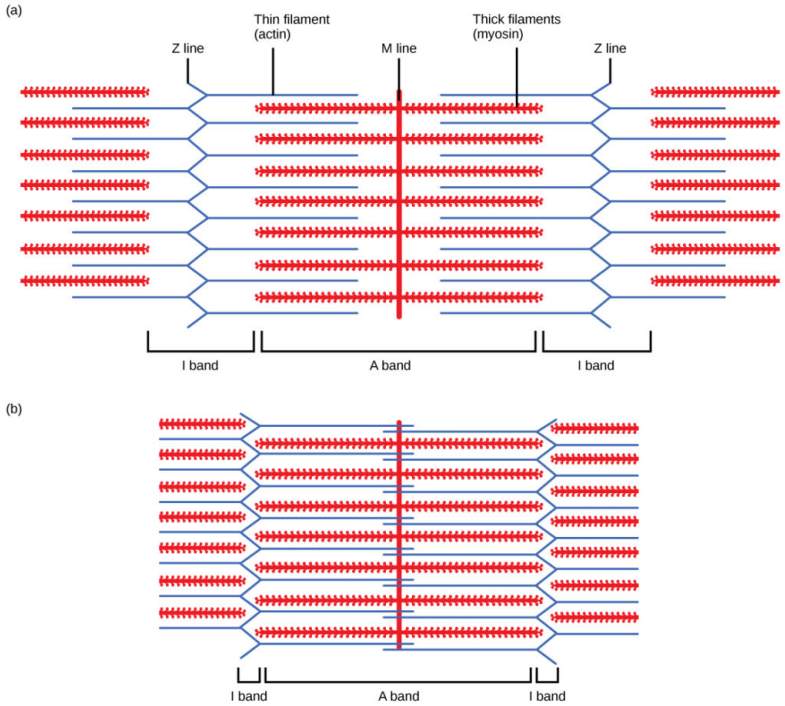

Figure 2.3: The sarcomere during relaxation (a) and contraction (b) [13].

2.1.1 Trapezius Muscle

The trapezius muscle is a large, superficial muscle that covers most of the upper back, extending from the occipital bone to the lower thoracic vertebrae of the spine as shown in Figure 2.4. The trapezius contains three functional regions. The upper trapezius is used to support the weight of the arm, extend the neck, and medially rotate the scapula. The transverse trapezius stabilizes and retracts the scapula, while the lower trapezius medially rotates and depresses the scapula [14]. In addition to providing support and mobility to the arms, neck, and scapula, the trapezius plays an important role in supporting the spine, allowing the spinal column to stay erect while in a standing position.

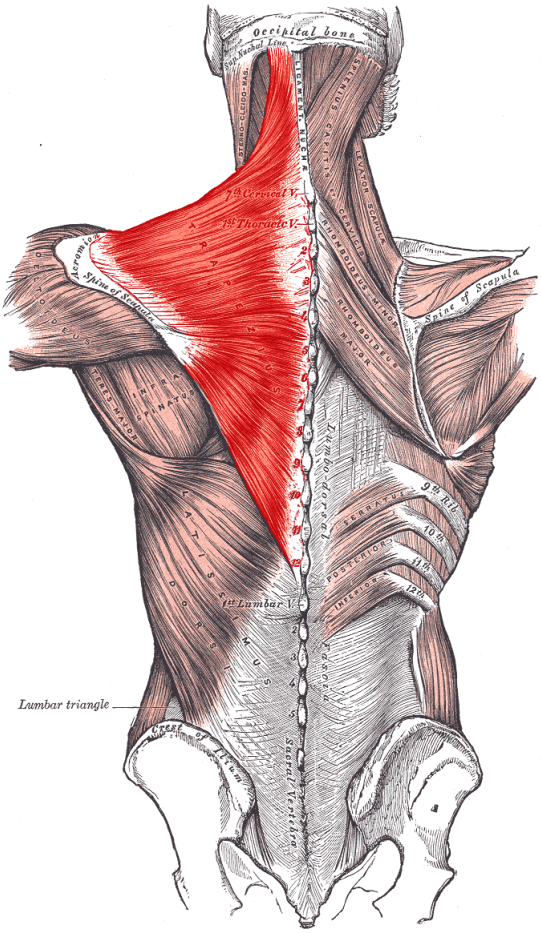

Figure 2.4: The location of the trapezius muscle.

2.2 Chronic Pain

Chronic pain is the terminology usually used to describe any pain that has lasted for longer than three months. Because pain is a subjective experience, it is difficult to consistently rate pain. Everyone experiences pain differently, from their sensitivity to pain, to their sensation felt as pain. This creates difficulties when trying to assess pain across patient populations. The most common form of rating pain is to use a simple 0-10 rating scale of pain severity though, several other rating methods exist. Each of these assessments is completed using a checklist of observations and objective measurements to identify signs of pain. Examples are the Brief Pain Inventory and the Mankoski and McGill Pain Scales which are questionnaires completed by the patient. Each questionnaire has the patient describe their pain symptoms, how they experience their pain, and how their pain affects their daily life.

2.2.1 Myofascial Pain Syndrome

Myofascial pain syndrome (MPS) is the most common chronic pain disorder. MPS affects the fascia of the skeletal muscles in the neck, shoulders, and upper and lower back but, can cause pain throughout the body in a process known as referred pain. While common, the condition is poorly understood with no known etiology or pathophysiology. Even within the pain community, there is no consensus on the diagnostic criteria. The most agreed upon criteria deemed to be either essential to, or associated with, MPS are tender spots causing local pain, recognition of symptoms upon palpation of the site, and taut bands of muscle as described in Table 2.1 [6].

2.2.2 Myofascial Trigger Points

A frequent finding in sufferers of MPS are myofascial trigger points (MTrPs), visualized in Figure 2.5. The most common definition of MTrPs is that they are tender, taut, palpable nodules that can form in skeletal muscle, notably meeting most of the criteria in Table 2.1. MTrPs come in two varieties, active MTrPs (A-MTrPs) which cause spontaneous pain [10],

Table 2.1: Palpatory findings of MPS [6].

	Essential	**Associated**	**Irrelevant**	**Exclusionary**
Tender spot causing local pain*	148 (72%)	48 (23%)	9 (4%)	2 (1%)
Recognition of symptoms upon palpation of tender spot*	117 (58%)	72 (35%)	12 (6%)	1 (<1%)
Taut band*	76 (36%)	118 (57%)	14 (7%)	0 (0%)
Tender spot referring pain or dysesthesia*	72 (35%)	122 (58%)	10 (5%)	3 (2%)
Tender nodule*	70 (34%)	115 (56%)	17 (8%)	4 (2%)
Tender nodule within taut band**	60 (29%)	123 (59%)	23 (11%)	1 (<1%)

Responses reported as n (%).
*>90% of respondents judges these to be "essential to" or "associated with" the diagnosis of MPS.
**>80% of respondents judged these to be "essential to" or "associated with" the diagnosis of MPS.

and latent MTrPs (L-MTrPs) which only cause pain upon palpation [11].

2.2.3 Diagnosis

MTrPs are recognizable within the muscle as a taut nodule during palpation of the tender site. Manual palpation and the response of the participant allows for the differentiation between A-MTrPs and L-MTrPs. L-MTrPs only produce a painful response upon palpation.

There is some debate as to whether the creation of a local twitch response is a necessary criteria for the diagnosis of a MTrP. A local twitch response is an involuntary, localized twitch only affecting the taut bands of skeletal muscle. The local twitch response is elicited through either the insertion of a needle into the taut band or by creating a snapping palpation where two fingers are placed over the taut band and slid away perpendicular to the muscle fiber orientation [16]. The local twitch response produces a measurable electrical response and has only been seen in muscle containing MTrPs.

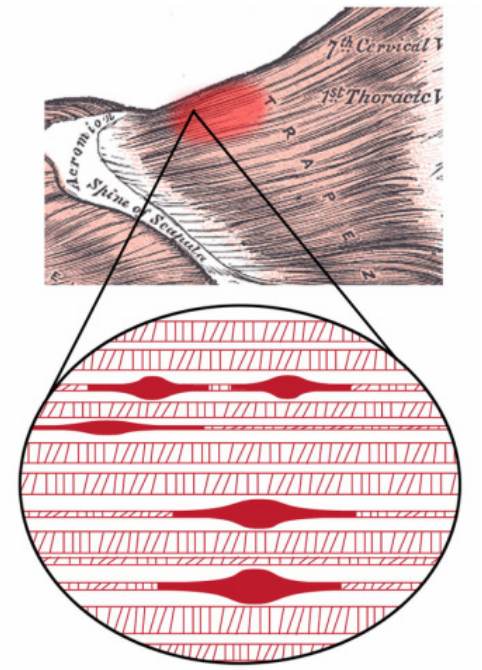

Figure 2.5: The taut muscle bands of a trigger point in the upper trapezius [15].

2.2.4 Pathology

The pathogenesis of MTrPs is currently unclear, but there are multiple proposed mechanisms, as described below, that could explain their development.

Energy Crisis Theory

The energy crisis theory is the idea that MTrPs are developed through an increase in the demand on the muscle. Macro-trauma or repetitive micro-trauma causes an increase in calcium release from the sarcolemma and prolonged shortening of the sarcomeres. A multitude of problems can predispose a person to microtrauma such as vitamin deficiencies, sleep disturbances, and lack of exercise [17]. This prolonged shortening diminishes the oxygen supply leaving the cells, preventing the production of ATP, a chemical necessary for muscular relaxation. The resulting buildup of metabolic waste could be responsible for the pain and tenderness.

This theory is supported by the number of individuals that develop MTrPs while maintaining occupations that require repetitive stress on a specific muscle [18]. Surgical scars and a variety of sports injuries caused by repetitive motions or spraining have also been shown to predispose a subject to the development of MTrPs [19].

Motor End-Plate Hypothesis

Studies have shown that MTrPs contain a point that creates characteristic electrical activity [20]. This point is frequently in the motor end-plate zone [21,22]. The activity created by the end-plate can be measured through electromyography (EMG) and is believed to represent increasing rates of release of acetylcholine from nerve terminals. This alone is not enough to explain the muscle contraction required for MTrP formation but, can co-exist with the energy crisis theory.

Radiculopathic Model

The radiculopathic model suggests that MTrPs are a secondary occurrence to a neurological condition [23, 24]. Gunn proposed that neural injury or compression could cause muscle spasms resulting in myofascial pain. This starts a snowballing effect leading to further neuropathy and degenerative changes in tendons and ligaments and perpetuates muscle shortening.

2.2.5 Treatments

Treatment for the management of MPS commonly focuses on the treatment of MTrPs [25]. However, many treatments for MTrPs are only supported by anecdotal evidence and are not conclusively shown to be effective, lacking any validation study. The following are treatments that have been investigated.

Massage Therapy

Some massage techniques are used to relieve headaches caused by referred pain from MTrPs. One study shows a decrease in headache frequency post-massage but, the results are identical to the control group that received the placebo treatment [26]. Another study included four test groups, a control group receiving a placebo treatment, a soft tissue massage group, a neural mobilization group, and a group which received a combination of soft tissue massage and neural mobilization treatment. This study found an increase in pain-pressure threshold in all non-placebo groups as well as, decreasing frequency, intensity, and punctuation. Results were improved in the combined treatment group [27]. Though a literature overview conducted by Maistrello *et al* suggests that there is little evidence for the usefulness of these treatments [28].

Stretching

The process of stretching the muscle containing the MTrP while topically applying either dichlorodifluoro-methane-trichloromonofluoromethane (Fluori-Methane) or ethyl chloride spray [17]. The sudden application of cold is believed to decrease pain sensitization while allowing for the muscle to be passively stretched to normal length [17].

Dry Needling

Dry needling, sometimes referred to as trigger point dry needling, is the repeated insertion of a solid filament needle into the MTrP. Multiple insertions may be done during a single session. The premise of this technique is that the advancement of the needle into the MTrP elicits a local twitch response in the muscle. These local twitch responses may help yield successful therapeutic outcomes for MTrP deactivation, possibly by disrupting the contracted musculature of the MTrP.

Gerber *et al* [29] conducted a study assessing the pain symptoms of subject's A-MTrPs before and after dry needling. This study concluded that dry needling reduces pain and can change MTrP status.

A second study was conducted by Gerber *et al* [30] assessed a patient's pain level and MTrP status before and after the dry needling of A-MTrPs, L-MTrPs, and normal muscle. It concluded that after a 6-week followup, a significant portion of patients had sustained improvement.

It is worth noting that the review of MTrP dry needling literature by Ong and Claydon found many studies inconclusive and called for further comparison of MTrP dry needling to placebo treatments [31].

Injection

MTrPs are identified using the same process as used in dry needling, but a hollow-bore needle is used instead to inject a solution into the MTrP. Lidocaine or procaine solutions are most frequently used for injection, but diclofenac, botulinum toxin type A, bupivacine, etidocaine, corticosteroids, and saline solutions have also been previously used. The patient may experience a soreness after injection depending on the solution injected or the needle gauge used. Thinner needles produce less soreness but, may prevent proper penetration of the needle into the MTrP. MTrP injection has been reported to have an immediate cessation or reduction of pain [32].

The improvement seen by MTrP injection is longer than the expected relief duration injected solutions. This suggests that there is an additional mechanism happening beyond the injection itself [33].

Electric Stimulation

Transcutaneous electrical nerve stimulation (TENS) is a therapy where electrodes are placed on the patient's body and a low-voltage electrical current is passed into their body. The electrodes are placed over MTrPs with the reasoning that they will stimulate the effected nerve fibers. It has been found that low frequencies ($<$50Hz) produced no pain relief while high frequencies ($>$50Hz) produced significant relief [34]. However, there was no change in the pain-pressure threshold.

Electroacupuncture is a combination of TENS and dry needling. It is the insertion of a pair of solid filament needles into the affected site, and then passing an electrical current through the needles. Ahmed *et al* suggests that electroacupuncture has much improved outcomes when compared to TENS [35].

Because there is no consensus on which of these approaches is the most beneficial for the treatment of MTrPs, I propose the use of medical imaging as a method to assess the clinical outcomes of these interventions and the affect they have on the musculature.

2.3 Imaging

Medical imaging is a term used to describe any modality used to view the human body with the purpose of diagnosing, monitoring, or treating medical conditions. Of these modalities, only magnetic resonance imaging (MRI) and ultrasound are safe, using only non-ionizing radiation, and are able to provide the contrast and resolution necessary to image musculature. The following is a review into these imaging modalities and their use in the examination of MPS and its characteristic MTrPs.

2.3.1 Magnetic Resonance Imaging

MRI is a noninvasive imaging modality that forms anatomical images through the use of powerful magnetic and radio-frequency (RF) fields. A magnet forces protons within the body to deviate from their equilibrium state and align in the direction of the magnetic field. An RF pulse is introduced which forces the protons to realign either 90° or 180° from the magnetic field. Once the RF pulse ends, the MRI's sensors are able to determine the amount of energy required for the protons to return to the alignment of the magnetic field.

Different settings of the MRI may be adjusted in order to affect the resulting scan. Repetition Time (TR) is the time between excitation of the same slice, and Echo Time (TE) is the time between the RF pulse and the peak of the signal. The two most common MRI imaging sequences are T1-weighted MRI which uses a short TR and TE, and T2-weighted MRI which uses a long TR and TE. Each method highlights different parts of the

body such as T1-weighted MRI being better for imaging fat while T2-weighted MRI can more visibly display edema. Several relevant studies have been conducted using MRI to image and evaluate muscle and MTrPs. Those most closely related to our proposed project are listed below.

Baraja-Vegas *et al* [36] used MRI to examine changes to the contractility of the gastrocnemius after dry needling L-MTrPs within the muscle. They used Short Tau Inverse Recovery (STIR), a form of fat-saturated T2-weighted MRI commonly used to detect muscle edema to identify swelling in the gastrocnemius while tensiomyography (TMG) was used to determine the gastrocnemius' contractility. Both MRI-STIR and TMG were preformed prior to, and one hour after, dry needling had occurred. Their results showed that post-dry needling, there was a significant increase in the MRI-STIR measurements for edema, increased muscle stiffness, and faster muscle contraction reaction times when compared to the non-needled control group.

Sollmann *et al* [37] used T2-weighted MRI to assess MTrPs in the upper trapezius of patients with migraines. T2-weighted MRI maps were created of the A-MTrPs. They found that the A-MTrPs contained significantly elevated T2 values when compared to the surrounding musculature.

Magnetic Resonance Elastography

Magnetic Resonance Elastography (MRE) is an extension of traditional MRI that can be used to measure tissue elasticity. MRE is conducted while a device emitting low-frequency vibrations is placed upon the patient in the scanner. The vibrations created by the device travel through the tissue, the velocity of which can be calculated. The velocity measurement can be used as a proxy measurement for tissue stiffness, with greater velocities indicating greater stiffness. Several studies have used MRE to examine muscle. Those relavant to this study are explained below.

Ito *et al* [38] created a novel MRE technique with the use of a vibration pad to allow for the simultaneous elastography of both the supraspinatus and trapezius muscles. The goal

of their study was to find a quantitative method of noninvasively determining stiffness for the purpose of diagnosis and treatment of rotator cuff tears. They found that the greatest imaging quality of the trapezius was achieved when the vibration pad was operated at 75Hz, while the supraspinatus improved in quality until 75Hz and then plateaued at higher frequencies.

Chen *et al* [39] used MRE to examine taut bands of muscle in the upper trapezius. This study involved patients with and without tant bands within the muscle. Each had MRE scans taken and the shear stiffness was calculated within the region of interest. The results indicate a higher stiffness around taut bands when compared to the surrounding muscle tissue, confirming the existence of taut bands of muscle identified by palpation.

2.3.2 Ultrasound

Ultrasound is a noninvasive imaging modality that can be used to produce images of the body through the use of high frequency sound waves. An ultrasound transducer contains individual elements made of piezoelectric material capable of emitting sound waves and detecting their reflection back. As emitted sound waves travel through tissue, any boundaries within the tissue or changes in tissue texture will result in a partial reflection of the sound wave. When the reflection returns to the transducer, the time passed since emission and the speed of sound through the medium are used to calculate the distance to where the reflection occurred.

The most basic form of ultrasound is called amplitude mode (A-Mode) and is created from the signal of an individual piezoelectric element. This is displayed as a 2-D plot where the y-axis represents depth into the tissue and the x-axis represents the intensity of the reflection received. The stronger the reflection, the higher the intensity, as shown in the left side of Figure 2.6.

The most common form of ultrasound is called brightness mode (B-Mode) which is created by combining the signals of an array of piezoelectric elements. The intensity of the A-Mode signal is converted into a brightness value, with higher values appearing brighter

and with each A-Mode signal forming a single scanline. An array of A-Mode scanlines is able to be converted into a 2-D B-Mode image where the x-axis is width and the y-axis is depth, as displayed on the right side of Figure 2.6. Ultrasound has been adapted to image muscle and has been previously used to examine MTrPs.

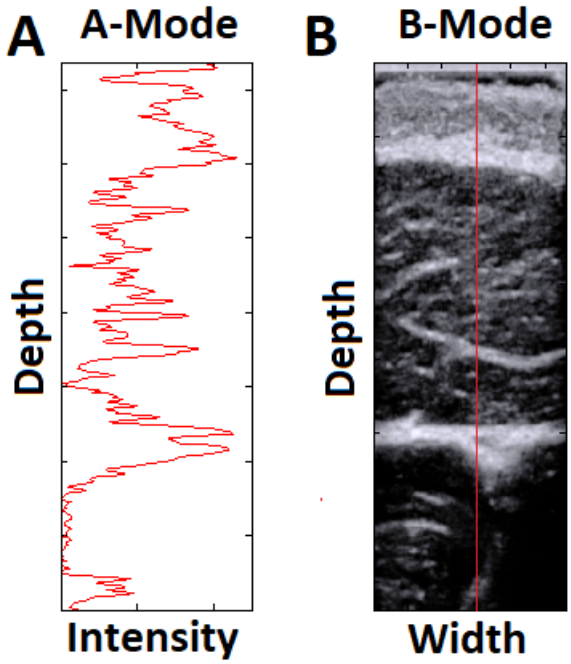

Figure 2.6: **A:** An A-Mode created from a single element in an ultrasound transducer. **B:** A B-Mode image comprised of many A-Modes put together. The A-Mode plot is taken from the red line in the B-Mode image.

Turo *et al* [40] used B-mode ultrasound to determine if texture-based analysis could differentiate between the structural heterogeneity of symptomatic MTrPs and normal muscle. Entropy filtering was performed on the B-Mode images and compared between L-MTrPs, A-MTrPs, and normal muscle. The results showed that A-MTrPs have lower entropy and, therefore, are more homogenous than normal muscle.

Though B-Mode is the most common form of ultrasound imaging, there are several ultrasound techniques that can be used to identify additional quantitative features of the images.

Doppler

Doppler is a form of ultrasound imaging that uses high-frequency sound to measure movement, traditionally from blood flow. If movement is occurring, the pulses emitted from the transducer will experience a phase shift. This technique has been previously used in the examination of MTrPs.

Sikdar *et al* [41] used Doppler ultrasound and compartment modeling to assess the velocity waveforms in blood vessels surrounding MTrPs. The preliminary findings suggest that A-MTrPs have higher peak systolic velocities and negative diastolic velocities compared to L-MTrPs and normal muscle.

Vibration Sonoelastography

Vibration Sonoelastography (VSE) is a form of ultrasound that makes use of an external vibration applying a harmonic signal to the surface of the tissue, inducing shear waves. The shear wave speed (SWS) can be measured in order to obtain the elasticity of the tissue. VSE has been previously used in the assessment of MTrPs.

Sidkar *et al* [42] used vibration sonoelastography (VSE) to examine L-MTrPs and A-MTrPs and normal muscle tissue. Each site was rated based upon its echogenicity and blood-flow waveform. This study concluded that A-MTrPs and L-MTrPs appear hypoechoic, suggesting a local change in tissue echogenicity. A-MTrPs were determined to have a higher blood-flow score when compared to L-MTrPs. This study was able to conclude that VSE can be used to distinguish between MTrPs and normal muscle.

Turo *et al* [43] used VSE and B-Mode Ultrasound to try and differentiate between A-MTrPs and normal muscle. They concluded that A-MTrPs have lower entropy when compared to normal muscle and that MTrPs are stiffer than normal muscle.

Turo *et al* [44] used VSE to examine A-MTrPs before and after dry needling treatment. This study found that among patients that responded to the treatment, the heterogeneity index was lower and even lower among the patient population with resolved MTrPs.

Sikdar *et al* [45] used VSE and B-Mode Ultrasound to examine MTrPs. The MTrPs

appeared as hypoechoic regions in the muscle. Spectral Doppler analysis showed lower vibration amplitudes within MTrPs compared to surrounding tissue. This suggests that MTrPs are hypoechoic and their stiffness can be quantified using ultrasound.

Ballyns *et al* [46] used VSE and Doppler on A-MTrPs, L-MTrPs, and palpably normal sites to determine whether any changes to the physical properties of the muscle occurred. The results showed that A-MTrPs were larger than L-MTrPs and palpably normal sites. Additionally an increase in blood vessel pulsatility occurred near A-MTrPs. This study concluded that MTrPs could be classified by area and that the pulsatility index may be a meaningful evaluation of MPS.

Supersonic Shear Imaging

Supersonic Shear Imaging (SSI) focuses multiple acoustic pulses together resulting in a conical shear wave. The shear wave is tracked using an ultrafast scanner allowing for the calculation of velocity and, therefore, elasticity. The use of SSI has been found to have applications in the examination of muscle.

Gennisson *et al* [47] used SSI to examine the viscoelastic and anisotropic properties of muscle tissue. By inducing a shear wave into the brachialis muscle they were able to map the elasticity of the muscle. Imaging occurred with increasing load placed on the brachialis muscle (0-5kg), and with the transducer being oriented either perpendicular or parallel to the muscle fibers. Their results show that increasing load on the muscle causes increased elastography values. Additionally, having the transducer aligned with the muscle fiber orientation results in much higher elastography values.

Shear Wave Elastography

Shear Wave Elastography (SWE) is an ultrasound method similar to SSI but instead of focusing multiple acoustic pulses, a single high intensity acoustic pulse is generated by the transducer. This pulse creates a perpendicular shear wave traveling through the tissue. By monitoring the shear wave, it is possible to calculate its speed. The speed of the shear wave

can be used to calculate the elasticity of the tissue. I believe that the use of shear wave elastography may be a useful tool for the examination of MTrPs.

Chapter 3: Methodology

3.1 Study Population

For this study, forty participates were recruited who exhibited chronic myofascial neck pain (>3 months). The George Mason University Review Board approved all study procedures.

3.2 Evaluation

Prior to imaging, subjects underwent a series of five tests carried out by a group of trained physicians. The combination of these tests allowed for the diagnosis of either normal, healthy muscle tissue or a MTrP, and the further differentiation between an A-MTrPs or L-MTrPs.

3.2.1 Written Self Evaluation

Each subject completed the necessary paperwork prior to beginning any experimentation.

The Brief Pain Inventory was used to identify the severity of any current pain, its location, as well as, how the pain affects well-being such as mood, relationships, ability to sleep, and ability to walk. The Brief Pain Inventory is also used to identify what causes a worsening of the pain, and what, if anything, causes relief from the pain.

The Beighton Scale is used as a measurement for hypermobility in the subject's joints. This is a binary rating system indicating whether the elbow and knee joints can hyperextend beyond 10°, whether the fifth finger is capable of passive dorsiflexion beyond 90°, or if the thumb is able to dorsiflex to the flexor aspect of the forearm. A final test is conducted by having the subject bend and rest their palms flat on the floor with their knees fully extended. The results are scored between 0-9.

The next test is the Brighton Score which is a continuation of the Beighton Scale. Points are accumulated for joint pain, varicose veins, abnormal skin, and having Marfanoid habitus body type (having especially long extremities) among other things. These points are added to the previous score received from the Beighton Scale for a total assessment score of the subject's hypermobility. The final scoring metric is a 19 point scale shown in Table 3.1.

Table 3.1: Brighton Score Classifications

Points	**Classification**
11-19	Severe
8-10	High
4-7	Moderate
2-3	Low
0-1	None

The Widespread Pain Index is used to score how widespread the subject's pain is across their body and the severity of that pain. The first section determines the extent of pain across the subject's body and is scored between 0-19, zero equates to no pain with 19 signifying wide-ranging pain across the body. Symptom severity is measured on a scale of 0-12. A zero represents no problem while 12 indicates a severe problem.

The final form was developed for this specific research project and contains two parts. The first part is completed by the subject and inquires which side of the neck the pain originates, how long the subject has had the pain, and what alleviates the pain. The second part is used by the physicians to record the results of the following tests.

3.2.2 Palpation

Trained physicians manually palpated the subject's neck and shoulders, shown in Figure 3.1, in order to identify tender sites or taut bands of muscle. Any taut bands were marked to clearly identify any areas for further examination.

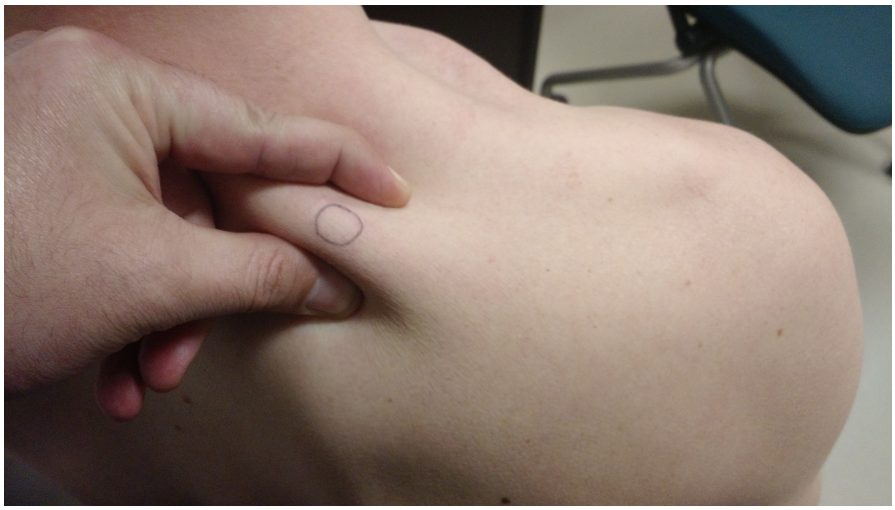

Figure 3.1: Palpation of the subject's upper trapezius in order to locate taut muscle bands. Once a taut muscle band is located, it is marked for easy identification.

3.2.3 Algometer

The algometer is a hand-held pressure measurement device, exhibited in Figure 3.2, used by the physician and placed on the neck or shoulder region of the subject. The physician applies increasing force to the subject through the algometer. The subject indicates when the applied force induces pain. The force required to illicit the painful response at that location is chronicled. This was repeated throughout the upper trapezius, focusing on the marked sites identified through palpation or the previously completed self evaluations. This is used to determine the subject's pain-pressure threshold.

3.2.4 Pin Prick Test

The pin prick test uses a series of seven needles of increasing weight (8mN, 16mN, 32mN, 64mN, 128mN, 256mN, 512mN). A sensitized location on the trapezius is selected and the smallest needle is gently lowered perpendicular to the skin until the tip of the needle makes contact. The needle does not penetrate the epidermis, instead its force is gently applied to the surface of the skin as demonstrated in Figure 3.3. After each application of the needle the subject indicates on a scale of 0-10 their level of discomfort and their response

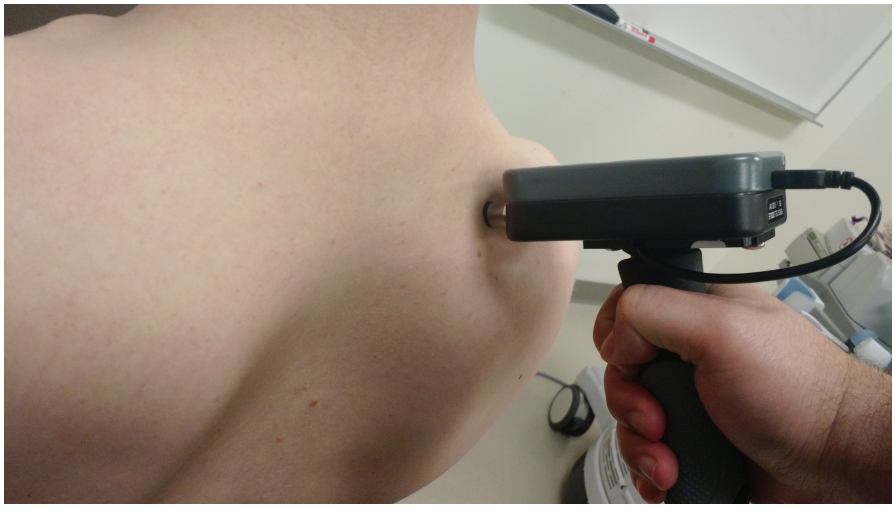

Figure 3.2: An algometer being used over a subject's marked site to determine the pain-pressure-threshold at that location.

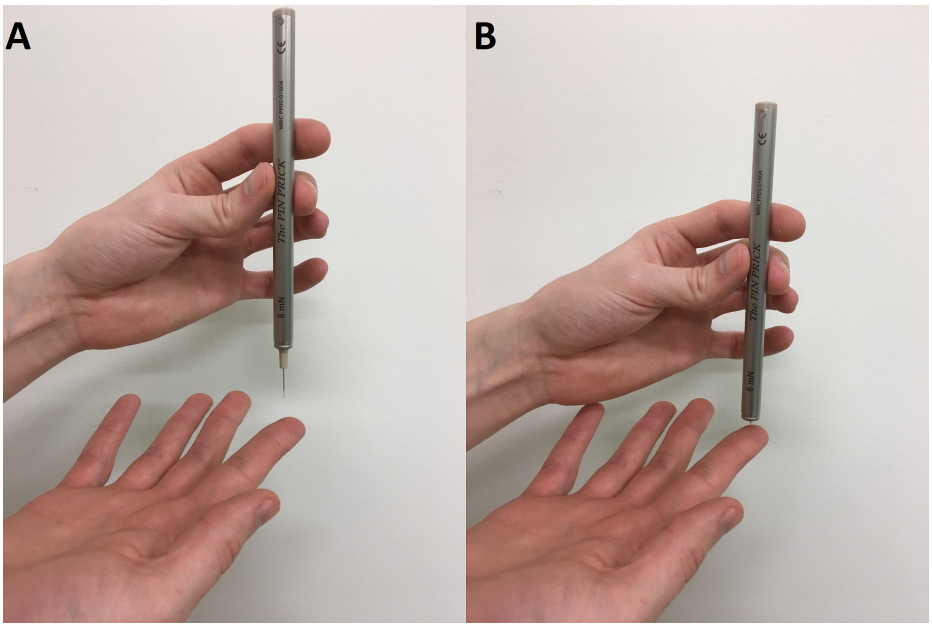

Figure 3.3: **A**: The 8mN needle fully extended. **B**: The 8mN needle gently lowered perpendicular to the skin's surface, causing the needle to retract inside its casing and applying the 8mN force to the contact point.

is recorded. Each needle application is repeated for a total of ten times, then reproduced with the next largest needle. This continues until all the needles are used or the subject is in too much discomfort to continue.

3.2.5 Cervical Range-Of-Motion (CROM) Assessment Device

The CROM is a device that is placed over the head that allows for the measurement of the range of motion of the cervical region. The CROM has three compasses that are placed on each plane around the subject's head; one on the top of the head, one of the forehead, and one over the left ear, as shown in Figure 3.4. The compasses are all guided by a pair of magnetic bars hung around the subject's neck; one in the front and one in the back creating a magnetic field around the subject. The subject is instructed to perform a series of motions

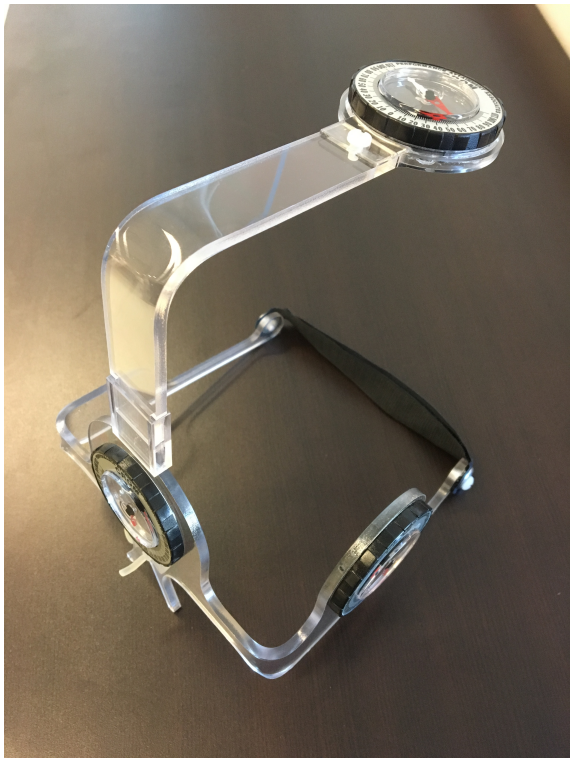

Figure 3.4: The CROM is placed over the subject's head and used to assessment their range of motion when performing occipital flexion and extension, lateral flexion, and cervical rotation.

while compass measurements are taken before and after each movement, allowing for the calculation of their range of motion. Subjects perform occipital flexion and extension, lateral flexion, and cervical rotation.

3.3 Imaging

3.3.1 Setup

Imaging was carried out using an Aixplorer Ultrasound System (SuperSonic Imagine, Aix en Provence, France) with an L10-2 linear array ultrasound probe while the subject was in a seated position. This system was used for both B-mode and SWE imaging. A custom made transducer holder, shown in Figure 3.5, was designed to enable the transducer to be held in place on the subject's body while allowing for rotation to precise angles in 10° intervals while imaging through a window with a diameter of 20mm.

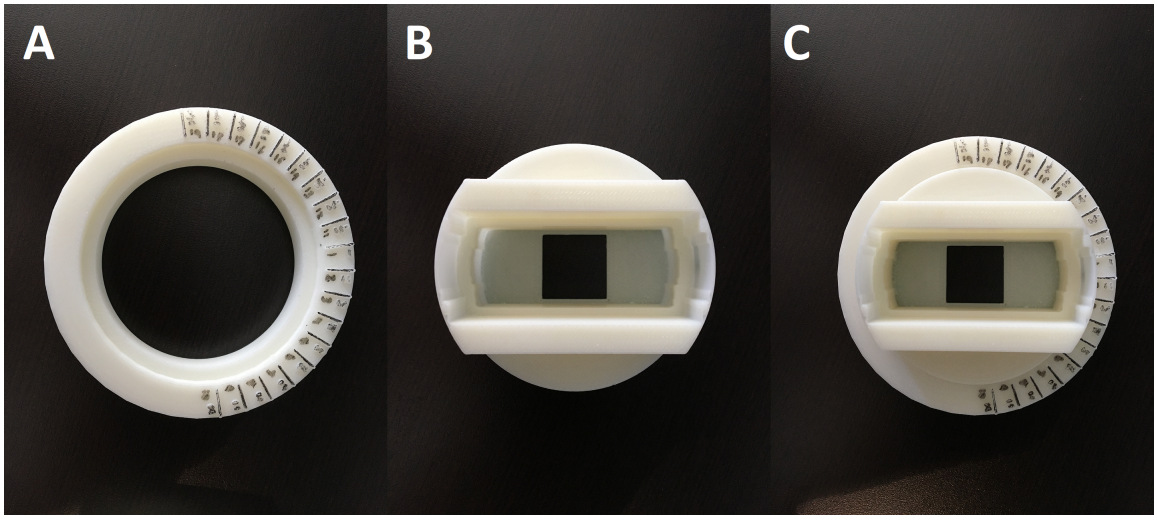

Figure 3.5: **A**: The outer ring of the transducer holder. This ring has a marker every 10° allowing for precise rotation of the inner ring. **B**: The inner ring where the transducer is held. The 10mm-by-10mm square cutout allowing for registration to a MTrP site is visible. **C**: The inner and outer rings combined.

3.3.2 Data Collection

The window of the transducer holder was placed over one of the sites marked on the subject's upper trapezius and held in place with adhesive while the 0° indicator marked the approximate muscle fiber orientation, as shown in Figure 3.7. This approximation was made by estimating a line between the acromioclavicular (AC) joint to the C7 spinous process on the spine, in the approximate direction of the fibers of the upper trapezius, as demonstrated in Figure 3.6. This registers the marked site to the B-mode and SWE images.

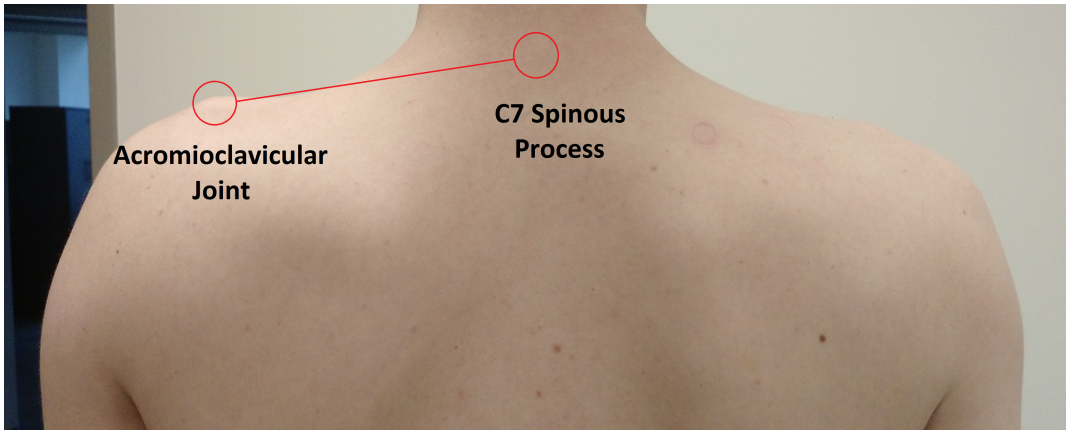

Figure 3.6: In order to establish transducer probe orientation, the approximate orientation of the muscle fibers of the upper trapezius is determined by imagining a line connecting the acromioclavicular joint and the C7 spinous process.

The ultrasound machine was then turned to the SWE imaging mode and the custom probe holder turned to -90°. After a several second pause that allows the low frame rate of the SWE imaging to properly measure the tissue within the imaging window, an image is saved and the probe is then rotated clockwise 10°. This is repeated for a total of nineteen images.

3.4 Processing

After the data collection, the file containing all of the saved images from that session was opened on the ultrasound machine and the built-in Q-box tool was used. This tool allows

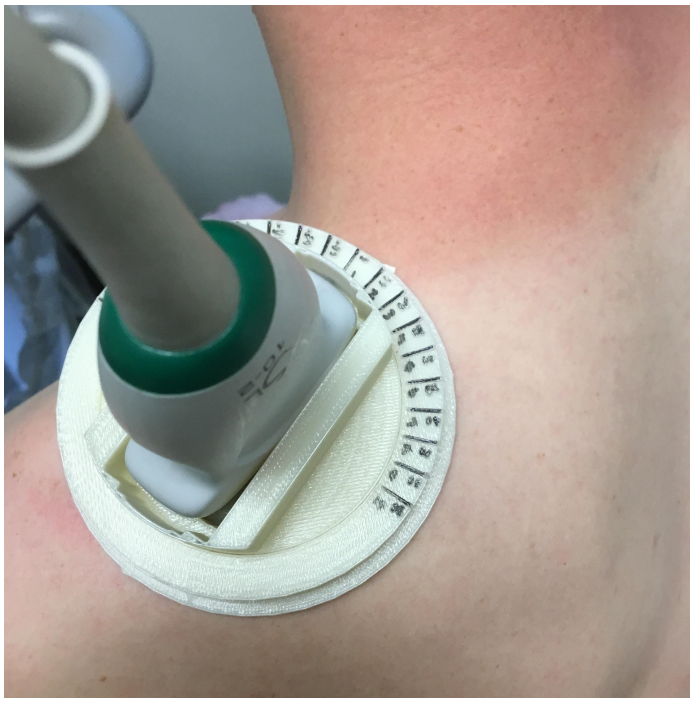

Figure 3.7: Custom Probe holder mounted on the shoulder with transducer inserted and aligned to 0°, the approximate alignment of the muscle fiber orientation.

for the selection of an region of interest (ROI) within the SWE images and calculates the average SWE value within the ROI. Two measurement options are available: velocity (m/s), and shear modulus (kPa). Velocity is the direct measurement, while the shear modulus is calculated using Equation 3.1 where μ is the shear modulus, ρ is the tissue density, and V is the shear wave velocity. The velocity measurement was used for all processing due to being the direct measurement.

$$\mu = \rho \times V^2 \tag{3.1}$$

The Q-box ROI was used to select the largest possible region of the trapezius without exceeding its upper and lower boundaries, exemplified in Figure 3.8. Each of the 19 images per marked site was converted into nineteen corresponding velocity measurements. These measurements were then transferred to MATLAB for further analysis. The velocity

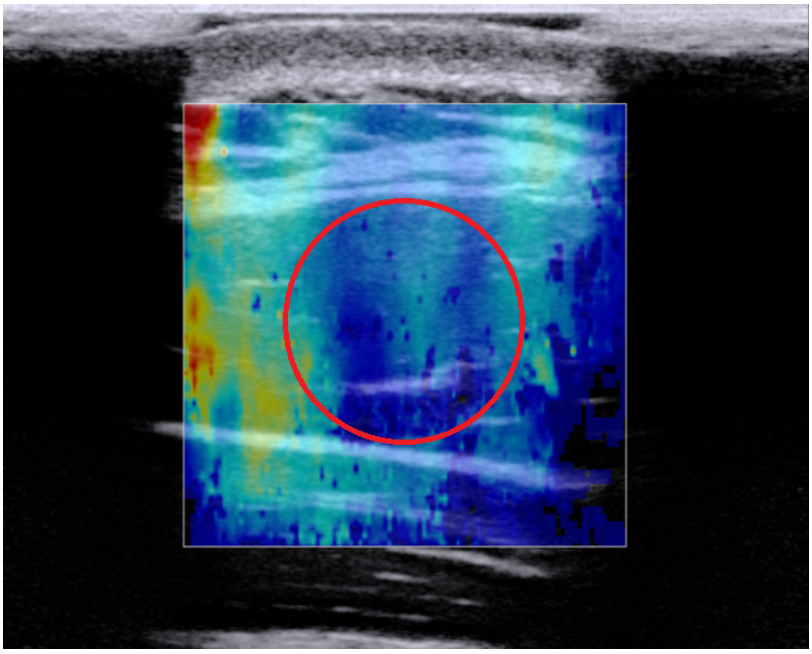

Figure 3.8: The Q-box tool is used to highlight the muscle within the trapezius. Once the ROI is selected, the average shear wave speed within that region is the output.

measurements were input into an array. This array was rotated until the greatest velocity measurement was in the center, corresponding to the true muscle fiber orientation. These values were then interpolated and plotted against angle in degrees relative to the muscle fiber orientation from -90° to 90°. From here, two different metrics were created and used in order to evaluate the asymmetry of the plot, shown in **A** of Figure 3.9.

The first asymmetry metric determined the full width at half maximum (FWHM) using Equation 3.2 for each of the labeled sites. The FWHM line was horizontally plotted across the initial curve as shown in **B** of Figure 3.9. Then a vertical line was overlaid through the maximum value of the plot denoting the estimated true fiber orientation. This allowed for the identification of the intersections of the horizontal FWHM line and the initial curve. The difference between the left intersect and the center line was determined and subtracted from the difference between the right intersect and the center line using Equation 3.3. The resulting absolute value was determined to be the asymmetry value for that site measured in degrees.

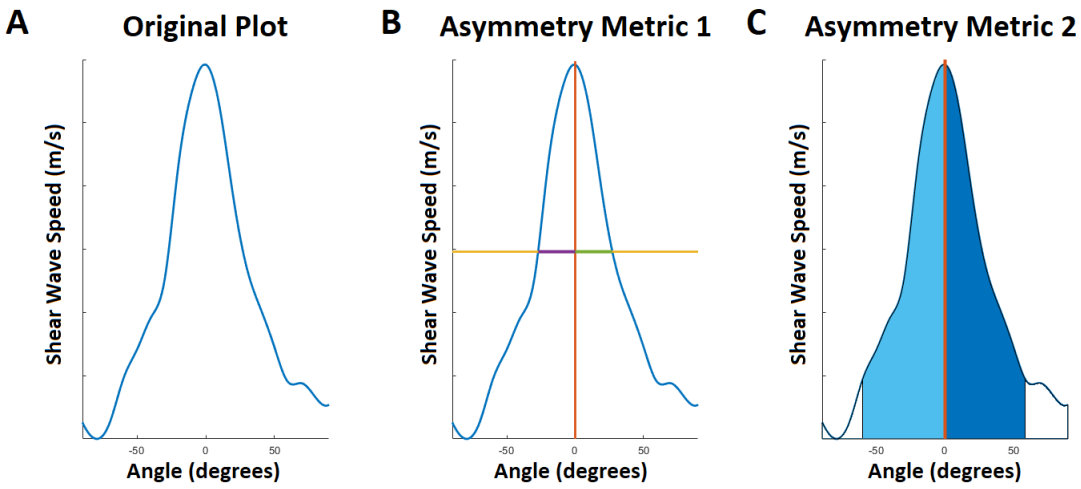

Figure 3.9: **A:** An example of the interplated data from which the asymmetry value would be determined. **B:** An example of how asymmetry is calculated using the first metric. The blue line represents the original plot, yellow is the vertical line through the plot's peak value, orange is the horizontal FWHM value, purple is the difference between the center line and the left intersect of the FWHM line and original plot, green is the difference between the right intersect of the original plot and FWHM line. The absolute difference between the purple and green lines would be the asymmetry value using metric 1. **C:** An example of how the second asymmetry metric is calculated. The plot is divided in half based on the location of the maximum value. The areas under the curve 60° to the left of center (light blue) and 60° to the right of center (dark blue) are calculated and the difference is taken. The absolute difference is the asymmetry value for metric 2.

$$FWHM = \frac{X_{max} - X_{min}}{2} + X_{min} \tag{3.2}$$

$$\text{Asymmetry} = |(\text{Right Intersection - Center}) - (\text{Center - Left Intersection})| \tag{3.3}$$

The second asymmetry metric begins by dividing the plots in half based on the location of the maximum SWS value. The area under the curve of the left and right sides was calculated using Equation 3.4. To account for any error that may have occurred as a result of the plot having been rotated to ensure that the peak value was in the center, the area

under the curve was only calculated for 60° to the right and left of the center as shown in **C** of Figure 3.9. The absolute difference between the two areas was taken as the asymmetry value.

$$Asymmetry = |\int_{-60}^{0} f(x)dx - \int_{0}^{60} f(x)dx| \tag{3.4}$$

3.5 Analysis

The absolute asymmetry values for normal muscle tissue, L-MTrPs, and A-MTrPs were separated and their statistical significance was determined using a heteroscedastic two-tailed Student's t-test. The same comparison was made between normal muscle tissue and a combined group of L-MTrPs and A-MTrPs.

Chapter 4: Results

In the study population of 40 subjects, we imaged a total of 79 marked sites. Of these sites, five sites were excluded from analysis due to overlapping diagnostic criteria. One normal site was removed from analysis due to its poor image quality resulting in inconclusive results. In total we identified, imaged, and analyzed 40 A-MTrPs sites, 22 L-MTrPs sites, and 11 normal sites.

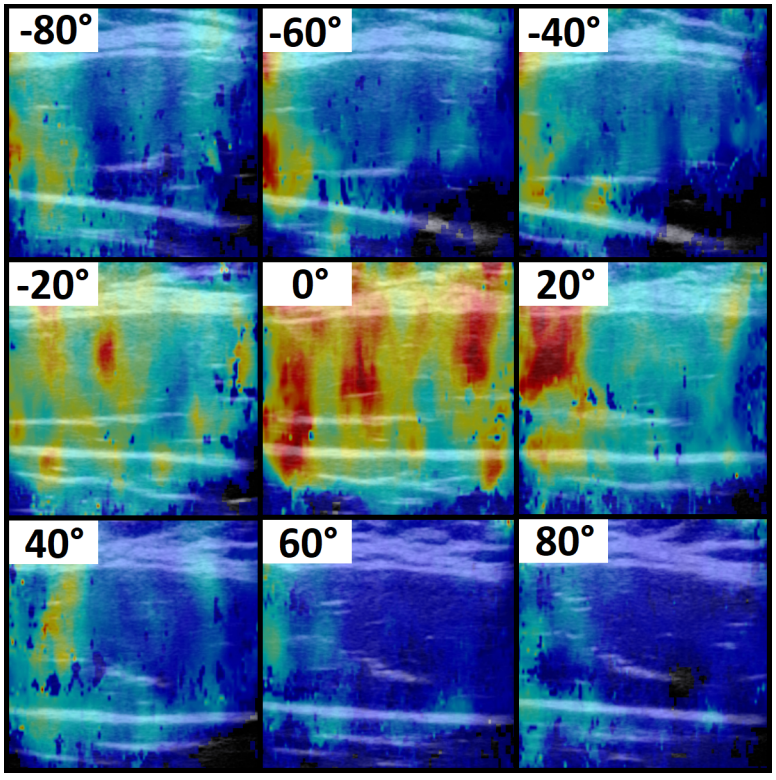

Figure 4.1: Demonstrates how SWE values increase as the transducer is rotated more in parallel with the muscle fiber orientation (0°) and decreases as the transducer is rotated back to perpendicular orientation to the muscle fiber (-90° and +90°).

We determined that in all cases the SWS changed with fiber orientation as expected, shown in Figure 4.1. When the SWS of normal muscle was plotted against transducer orientation, the result was an approximately bell-shaped curve. After analysis, plots representing symptomatic sites were shown to have a greater average asymmetry value when compared to normal muscle sites, as shown in Table 4.1 and illustrated in Figure 4.2. The results of the Student's t-test comparison found a statistically significant difference between normal muscle tissue and A-MTrPs as shown in Table 4.2. The difference between normal muscle tissue and A-MTrPs was found to be statistically significant.

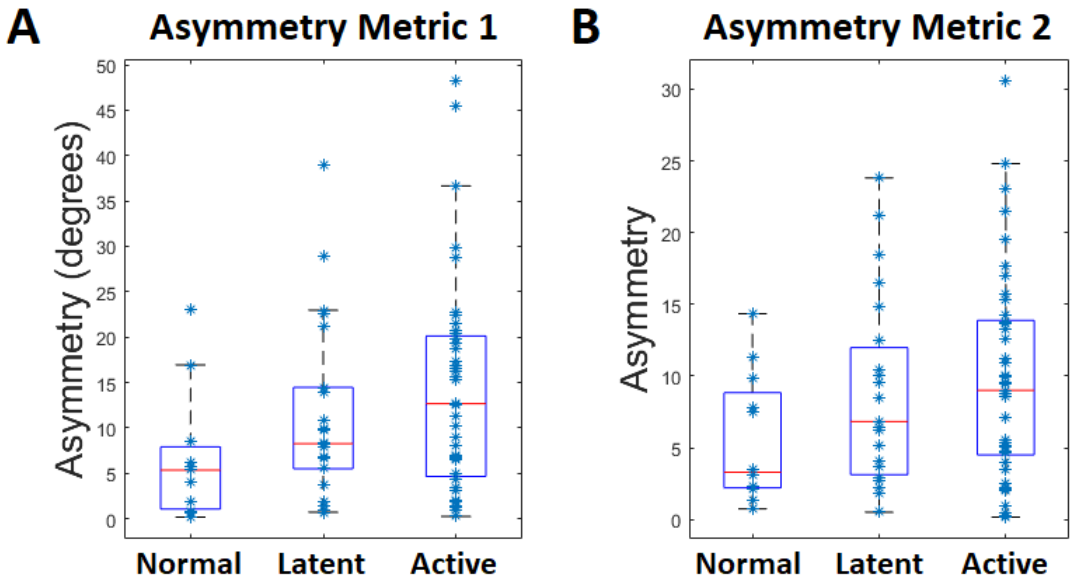

Figure 4.2: Displays the muscle asymmetry distribution of each of the three groups: normal muscle, latent trigger points, and active trigger points. **A** shows the results from the first asymmetry metric which compared the distances from the center to the left and right intersects of the FWHM line. **B** shows the second metric which compared the area under the curve of the left and right sides of the plot.

Table 4.1: Average Asymmetry and Standard Deviation of Fiber Orientation

Muscle Condition	**Metric 1: Asymmetry (°) (Mean ± STD)**	**Metric 2: Asymmetry (°) (Mean ± STD)**
Normal (N = 11)	6.64 ± 7.23	5.59 ± 4.45
Latent (N = 22)	11.51 ± 9.86	8.62 ± 6.51
Active (N = 40)	14.19 ± 11.76	9.87 ± 7.31

Table 4.2: Results of T-Test Comparison

t-Test	**Metric 1: p-value**	**Metric 2: p-value**
Normal-MTrP	0.01968	0.02361
Normal-Latent	0.11992	0.11528
Normal-Active	0.01393	0.02096
Latent-Active	0.34417	0.51745

Chapter 5: Discussion

The results of this study indicate that the variation of the SWS with transducer orientation is asymmetric in the case of muscle containing A-MTrPs. A likely explanation for this observation is that the fiber orientation in the case of muscle containing A-MTrPs is more heterogeneous than palpably normal muscle. If all muscle fibers were orientated in one direction parallel to each other, the plot of shear speed against transducer orientation would have been perfectly symmetric. Because mirrored orientations of the transducer with respect to the muscle (e.g. -45° and +45°) would lead to identical relative alignments with respect to the fibers and correspondingly lead to similar values of measured shear speed, visualized by **A** in Figure 5.1. However, with the introduction of a palpable, symptomatic site, the muscle fiber orientation becomes disrupted resulting in unique measurements at mirrored transducer orientations, exemplified in **B** of Figure 5.1. We conclude this to be the source of the asymmetry observed in our study.

MTrPs present as physically palpable, tender nodules, located within the skeletal muscle. MTrPs were previously hypothesized to be a local contracture within the muscle or associated with abnormalities within the fascial boundary [44]. Muscle contracture semi-permanently shortens the muscle and causes changes in the fiber orientation. Thus, local contractures caused by the introduction of an MTrP could cause disruption in the local fiber orientation. In previous work, it was observed that MTrPs appeared hypoechoic and did not support a propagating vibration when imaged with VSE. Similar findings were also noted during SWE imaging. A local disruption of the muscle fiber architecture could be an important feature distinguishing A-MTrPs from normal muscle tissue. Our results show that normal muscle tissue may also be distinguishable from L-MTrPs. However, these differences were not statistically significant at our sample size.

These results are consistent with the previous work carried out Turo *et al* that found

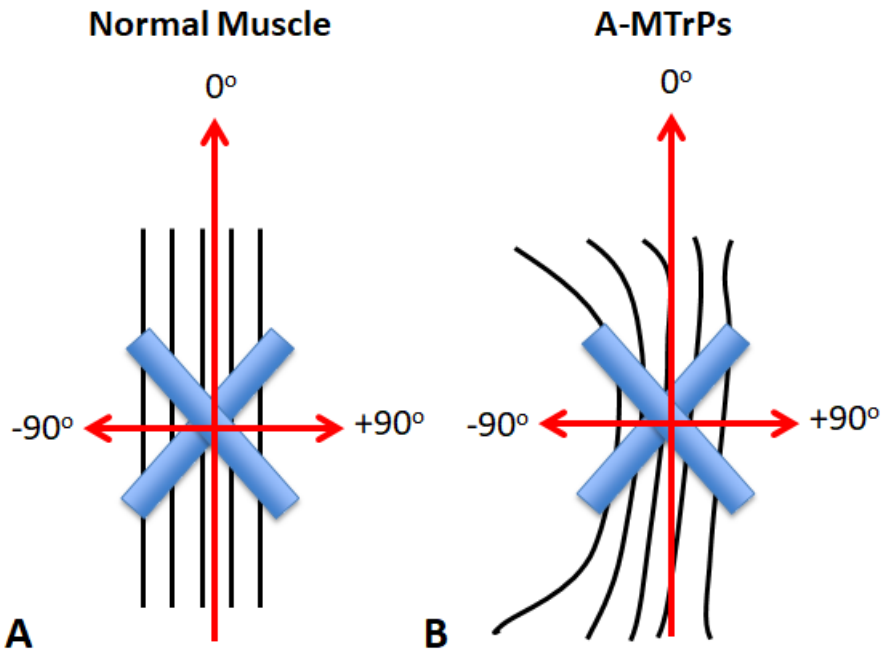

Figure 5.1: A hypothetical model that could explain the observed asymmetry in shear speed as a function of transducer orientation when imaging MTrPs. **A**: The muscle fibers (black lines) are all aligned. The placement of the transducer (blue rectangles) at symmetric angles around 0° leads to identical SWS measurements. **B**: The introduction of a MTrP disrupts the muscle fiber alignment. Identical placement of the transducer around 0° results in different SWS measurements.

heterogeneous mechanical properties in muscles with A-MTrPs [44]. Some histological studies have suggested that muscle fiber architecture in MTrP regions is disrupted although, these findings have not been widely reproduced [48].

In our study, two different metrics to measure muscle fiber asymmetry were used. While both metrics resulted in the same trend of more symptomatic sites having higher asymmetry values, the second metric comparing the area under the curve of the left and right sides proved to be more robust. This is due to the second metric being able to provide differentiation between normal muscle, L-MTrPs, and A-MTrPs, while also having a lower percent deviation.

5.1 Limitations

This study was conducted with several limitations that need to be acknowledged. The first limitation is the small sample size. While finding participants for examination, we only sought those who suffer from chronic neck pain with at least one A-MTrP or L-MTrP. The only times we were able to acquire healthy muscle images was when the patient was only symptomatic on one side of their body. If the physicians assessment showed that the subject had MTrPs on only one side of their trapezius, we would image the opposite trapezius to acquire healthy muscle data. Due to the lack of patients that were symptomatic on only one side, and healthy subjects not being included in the study, we had few healthy muscle sites to measure, a number which ceased growing early into the study. The small population of healthy muscle sites is something that could have been prevented with the inclusion of a healthy patient population.

Another weakness of this study was the SWE measurement. While SWE provides quantitative measurements of tissue stiffness, it can provide irreproducible measurements when performed with direct application of the transducer to the skin surface, as the application of any force to the tissue will result in a change in the SWS measurement [49]. This could have been prevented with the use of a standoff layer of ultrasound gel. However, this would have made orientating the transducer to precise angles a much more difficult task.

Finally, during the analysis of the data, an assumption was made that the peak SWS value in each data set represented the true muscle fiber orientation. Even though this was a fair assumption based on the research of Gennisson *et al* [47], we are unable to ensure its absolute precision.

5.2 Future Work

Continued work on this project would seek to both deepen the understanding of our findings and address the aforementioned issues. Further investigations would be carried out with

a larger subject population and with the inclusion of a larger control population. Additionally, the validation of the SWS results of our study in a setting where the muscle fiber orientation could be altered would help to confirm our results. This could be carried out in combination with a systematic reproducibility assessment of our anisotropy measurements with the use of High Angular Resolution Diffusion Imaging (HARDI), a form of MRI capable of noninvasively determining true muscle fiber orientation. With this we would be able to confirm both the true fiber orientation and definitively determine if muscle fiber asymmetry is occurring in muscle containing MTrPs. Finally, continued refinement and improvement of the asymmetry metric could allow for a more precise measurement and differentiation between symptomatic and asymptomatic groups.

The next step in continuing this work would be to use the technique we have developed to assess subjects before and after they have received treatment. I would hypothesize that if the subject experiences relief from MPS symptoms post-treatment that the asymmetry value would have decreased between measurements.

5.3 Conclusion

This study proposes an objective, quantitative measurement of the mechanical properties of anisotropic muscle with the use of shear wave elastography. The imaging protocol using a custom transducer holder allowed for the careful alignment of the imaging window over any palpable findings. Of the groups assessed, normal muscle was shown to have the lowest asymmetry value (5.59 ± 4.45), while muscle containing L-MTrPs (8.62 ± 6.51) and A-MTrPs (9.87 ± 7.31) have much larger values. Our results demonstrate that this measurement can be used to distinguish between symptomatic and asymptomatic sites ($p<0.024$). Further distinction can be shown between normal muscle and muscle containing A-MTrPs ($p<0.021$).

Bibliography

[1] J. Pergolizzi, K. Ahlbeck, D. Aldington, E. Alon, F. Coluzzi, A. Dahan, F. Huygen, M. Kocot-Kpska, A. C. Mangas, P. Mavrocordatos, B. Morlion, G. Mller-Schwefe, A. Nicolaou, C. Prez Hernndez, P. Sichre, M. Schfer, and G. Varrassi, "The development of chronic pain: physiological CHANGE necessitates a multidisciplinary approach to treatment," *Current Medical Research and Opinion*, vol. 29, no. 9, pp. 1127–1135, Sep. 2013. [Online]. Available: https://www.ncbi.nlm.nih.gov/pmc/articles/PMC3793283/

[2] D. J. Gaskin and P. Richard, "The economic costs of pain in the United States," *The Journal of Pain: Official Journal of the American Pain Society*, vol. 13, no. 8, pp. 715–724, Aug. 2012.

[3] N. Hendler, "Why Chronic Pain Patients are Misdiagnosed 40 to 80% of the Time?" *Journal on Recent Advances in Pain*, vol. 2, no. 3, pp. 94–98, 2016. [Online]. Available: http://www.jaypeejournals.com/eJournals/ShowText.aspx?ID=10106&Type=FREE&TYP=TOP&IN=~/eJournals/images/JPLOGO.gif&IID=773&isPDF=YES

[4] I. Bergh, G. Steen, M. Waern, B. Johansson, A. Odn, B. Sjstrm, and B. Steen, "Pain and its relation to cognitive function and depressive symptoms: a Swedish population study of 70-year-old men and women," *Journal of Pain and Symptom Management*, vol. 26, no. 4, pp. 903–912, Oct. 2003.

[5] CDC, "Life expectancy at birth and at age 65, by sex: Organisation for Economic Co-operation and Development (OECD) countries, selected years 19802015," *New Zealand*, p. 2, 1990.

[6] W. E. Rivers, D. Garrigues, J. Graciosa, and R. N. Harden, "Signs and Symptoms of Myofascial Pain: An International Survey of Pain Management Providers and Proposed Preliminary Set of Diagnostic Criteria," *Pain Medicine*, vol. 16, no. 9, pp. 1794–1805, Sep. 2015. [Online]. Available: https://academic.oup.com/painmedicine/article/16/9/1794/1876647

[7] R. D. Gerwin, "Classification, epidemiology, and natural history of myofascial pain syndrome," *Current Pain and Headache Reports*, vol. 5, no. 5, pp. 412–420, Oct. 2001.

[8] D. G. Simons, J. G. Travell, and L. S. Simons, *Travell & Simons' Myofascial Pain and Dysfunction: Upper half of body.* Lippincott Williams & Wilkins, 1999, google-Books-ID: sU0XupX7DGsC.

[9] D. A. Fishbain, M. Goldberg, B. R. Meagher, R. Steele, and H. Rosomoff, "Male and female chronic pain patients categorized by DSM-III psychiatric diagnostic criteria," *Pain*, vol. 26, no. 2, pp. 181–197, Aug. 1986.

[10] C. Fernndez-de Las-Peas, D. Simons, M. L. Cuadrado, and J. Pareja, "The role of myofascial trigger points in musculoskeletal pain syndromes of the head and neck," *Current Pain and Headache Reports*, vol. 11, no. 5, pp. 365–372, Oct. 2007.

[11] K. R. Lucas, "The impact of latent trigger points on regional muscle function," *Current Pain and Headache Reports*, vol. 12, no. 5, pp. 344–349, Oct. 2008.

[12] "Skeletal Muscle Anatomy and Physiology." [Online]. Available: https://opentextbc.ca/anatomyandphysiology/chapter/10-2-skeletal-muscle/

[13] "Sliding Filament Model of Contraction | Biology for Majors II." [Online]. Available: https://courses.lumenlearning.com/wm-biology2/chapter/sliding-filament-model-of-contraction/

[14] J. Ourieff and A. Agarwal, "Anatomy, Back, Trapezius," in *StatPearls*. Treasure Island (FL): StatPearls Publishing, 2018. [Online]. Available: http://www.ncbi.nlm.nih.gov/books/NBK518994/

[15] "Myofascial Trigger Point Therapy." [Online]. Available: http://www.jenniferparmenter.com/myofascial-trigger-point-therapy.html

[16] C.-Z. Hong, "Persistence of local twitch response with loss of conduction to and from the spinal cord," *Archives of Physical Medicine and Rehabilitation*, vol. 75, no. 1, pp. 12–16, Jan. 1994. [Online]. Available: https://www.archives-pmr.org/article/0003-9993(94)90330-1/abstract

[17] S. C. Han and P. Harrison, "Myofascial pain syndrome and trigger-point management," *Regional Anesthesia and Pain Medicine*, vol. 22, no. 1, pp. 89–101, Jan. 1997. [Online]. Available: http://www.sciencedirect.com/science/article/pii/S1098733906800623

[18] E. Rachlin and I. Rachlin, *Myofascial Pain and Fibromyalgia*. Elsevier, 2002. [Online]. Available: https://linkinghub.elsevier.com/retrieve/pii/B9780323011556X50014

[19] A. A. Fischer, "Injection techniques in the management of local pain," *Journal of Back and Musculoskeletal Rehabilitation*, vol. 7, no. 2, pp. 107–117, Jan. 1996.

[20] D. R. Hubbard and G. M. Berkoff, "Myofascial trigger points show spontaneous needle EMG activity," *Spine*, vol. 18, no. 13, pp. 1803–1807, Oct. 1993.

[21] D. G. Simons, "Do endplate noise and spikes arise from normal motor endplates?" *American Journal of Physical Medicine & Rehabilitation*, vol. 80, no. 2, pp. 134–140, Feb. 2001.

[22] D. G. Simons, C.-Z. Hong, and L. S. Simons, "Endplate potentials are common to midfiber myofacial trigger points," *American Journal of Physical Medicine & Rehabilitation*, vol. 81, no. 3, pp. 212–222, Mar. 2002.

[23] C. C. Gunn, "Radiculopathic Pain: Diagnosis and Treatment of Segmental Irritation or Sensitization," *Journal of Musculoskeletal Pain*, vol. 5, no. 4, pp. 119–134, Jan. 1997. [Online]. Available: https://doi.org/10.1300/J094v05n04_11

[24] J. L. Quintner and M. L. Cohen, "Referred pain of peripheral nerve origin: an alternative to the "myofascial pain" construct," *The Clinical Journal of Pain*, vol. 10, no. 3, pp. 243–251, Sep. 1994.

[25] L. Tekin, S. Akarsu, O. Durmu, E. Cakar, U. Diner, and M. Z. Kralp, "The effect of dry needling in the treatment of myofascial pain syndrome: a randomized double-blinded placebo-controlled trial," *Clinical Rheumatology*, vol. 32, no. 3, pp. 309–315, Mar. 2013.

[26] A. F. Moraska, L. Stenerson, N. Butryn, J. P. Krutsch, S. J. Schmiege, and J. D. Mann, "Myofascial trigger point-focused head and neck massage for recurrent tension-type headache: a randomized, placebo-controlled clinical trial," *The Clinical Journal of Pain*, vol. 31, no. 2, pp. 159–168, Feb. 2015.

[27] A. Ferragut-Garcas, G. Plaza-Manzano, C. Rodrguez-Blanco, O. Velasco-Roldn, D. Pecos-Martn, J. Oliva-Pascual-Vaca, B. Llabrs-Bennasar, and . Oliva-Pascual-Vaca, "Effectiveness of a Treatment Involving Soft Tissue Techniques and/or Neural Mobilization Techniques in the Management of Tension-Type Headache: A Randomized Controlled Trial," *Archives of Physical Medicine and Rehabilitation*, vol. 98, no. 2, pp. 211–219.e2, 2017.

[28] L. Falsiroli Maistrello, T. Geri, S. Gianola, M. Zaninetti, and M. Testa, "Effectiveness of Trigger Point Manual Treatment on the Frequency, Intensity, and Duration of Attacks in Primary Headaches: A Systematic Review and Meta-Analysis of Randomized Controlled Trials," *Frontiers in Neurology*, vol. 9, p. 254, 2018.

[29] L. H. Gerber, J. Shah, W. Rosenberger, K. Armstrong, D. Turo, P. Otto, J. Heimur, N. Thaker, and S. Sikdar, "Dry Needling Alters Trigger Points in the Upper Trapezius Muscle and Reduces Pain in Subjects With Chronic Myofascial Pain," *PM & R: the journal of injury, function, and rehabilitation*, vol. 7, no. 7, pp. 711–718, Jul. 2015.

[30] L. H. Gerber, S. Sikdar, J. V. Aredo, K. Armstrong, W. F. Rosenberger, H. Shao, and J. P. Shah, "Beneficial Effects of Dry Needling for Treatment of Chronic Myofascial Pain Persist for 6 Weeks After Treatment Completion," *PM & R: the journal of injury, function, and rehabilitation*, vol. 9, no. 2, pp. 105–112, 2017.

[31] J. Ong and L. S. Claydon, "The effect of dry needling for myofascial trigger points in the neck and shoulders: a systematic review and meta-analysis," *Journal of Bodywork and Movement Therapies*, vol. 18, no. 3, pp. 390–398, Jul. 2014.

[32] C. Z. Hong, "Lidocaine injection versus dry needling to myofascial trigger point. The importance of the local twitch response," *American Journal of Physical Medicine & Rehabilitation*, vol. 73, no. 4, pp. 256–263, Aug. 1994.

[33] S. R. Hameroff, B. R. Crago, C. D. Blitt, J. Womble, and J. Kanel, "Comparison of bupivacaine, etidocaine, and saline for trigger-point therapy," *Anesthesia and Analgesia*, vol. 60, no. 10, pp. 752–755, Oct. 1981.

[34] S. B. Graff-Radford, J. L. Reeves, R. L. Baker, and D. Chiu, "Effects of transcutaneous electrical nerve stimulation on myofascial pain and trigger point sensitivity," *Pain*, vol. 37, no. 1, pp. 1–5, Apr. 1989.

[35] S. Ahmed, C. Haddad, S. Subramaniam, S. Khattab, and D. Kumbhare, "The Effect of Electric Stimulation Techniques on Pain and Tenderness at the Myofascial Trigger Point: A Systematic Review," *Pain Medicine (Malden, Mass.)*, Jan. 2019.

[36] L. Baraja-Vegas, S. Martn-Rodrguez, F. Piqueras-Sanchiz, J. Faundez-Aguilera, I. J. Bautista, C. Barrios, and C. Fernndez-de-las Peas, "Localization of Muscle Edema and Changes on Muscle Contractility After Dry Needling of Latent Trigger Points in the Gastrocnemius Muscle," *Pain Medicine*, 2019. [Online]. Available: https://academic.oup.com/painmedicine/advance-article/doi/10.1093/pm/pny306/5305671

[37] N. Sollmann, N. Mathonia, D. Weidlich, M. Bonfert, S. A. Schroeder, K. A. Badura, T. Renner, F. Trepte-Freisleder, C. Ganter, S. M. Krieg, C. Zimmer, E. J. Rummeny, D. C. Karampinos, T. Baum, M. N. Landgraf, and F. Heinen, "Quantitative magnetic resonance imaging of the upper trapezius muscles - assessment of myofascial trigger points in patients with migraine," *The Journal of Headache and Pain*, vol. 20, no. 1, p. 8, Jan. 2019.

[38] D. Ito, T. Numano, K. Takamoto, T. Ueki, T. Habe, K. Igarashi, K. Mizuhara, and H. Nishijo, "Simultaneous acquisition of magnetic resonance elastography of the supraspinatus and the trapezius muscles," *Magnetic Resonance Imaging*, vol. 57, pp. 95–102, Apr. 2019. [Online]. Available: http://www.sciencedirect.com/science/article/pii/S0730725X18304417

[39] Q. Chen, J. Basford, and K.-N. An, "Ability of Magnetic Resonance Elastography to Assess Taut Bands," *Clinical biomechanics (Bristol, Avon)*, vol. 23, no. 5, pp. 623–629, Jun. 2008. [Online]. Available: https://www.ncbi.nlm.nih.gov/pmc/articles/PMC2474796/

[40] D. Turo, P. Otto, J. P. Shah, J. Heimur, T. Gebreab, K. Armstrong, L. H. Gerber, and S. Sikdar, "Ultrasonic tissue characterization of the upper trapezius muscle in patients with myofascial pain syndrome," *Conference proceedings: ... Annual International Conference of the IEEE Engineering in Medicine and Biology Society. IEEE Engineering in Medicine and Biology Society. Annual Conference*, vol. 2012, pp. 4386–4389, 2012.

[41] S. Sikdar, R. Ortiz, T. Gebreab, L. H. Gerber, and J. P. Shah, "Understanding the vascular environment of myofascial trigger points using ultrasonic imaging and computational modeling," *Conference proceedings: ... Annual International Conference of the IEEE Engineering in Medicine and Biology Society. IEEE Engineering in Medicine and Biology Society. Annual Conference*, vol. 2010, pp. 5302–5305, 2010.

[42] S. Sikdar, J. P. Shah, T. Gebreab, R.-H. Yen, E. Gilliams, J. Danoff, and L. H. Gerber, "Novel Applications of Ultrasound Technology to Visualize and Characterize Myofascial Trigger Points and Surrounding Soft Tissue," *Archives of physical medicine and rehabilitation*, vol. 90, no. 11, pp. 1829–1838, Nov. 2009. [Online]. Available: https://www.ncbi.nlm.nih.gov/pmc/articles/PMC2774893/

[43] D. Turo, P. Otto, J. P. Shah, J. Heimur, T. Gebreab, M. Zaazhoa, K. Armstrong, L. H. Gerber, and S. Sikdar, "Ultrasonic characterization of the upper trapezius muscle in patients with chronic neck pain," *Ultrasonic Imaging*, vol. 35, no. 2, pp. 173–187, Apr. 2013.

[44] D. Turo, P. Otto, M. Hossain, T. Gebreab, K. Armstrong, W. F. Rosenberger, H. Shao, J. P. Shah, L. H. Gerber, and S. Sikdar, "Novel Use of Ultrasound Elastography to Quantify Muscle Tissue Changes After Dry Needling of Myofascial Trigger Points in Patients With Chronic Myofascial Pain," *Journal of ultrasound in medicine : official journal of the American Institute of Ultrasound in Medicine*, vol. 34, no. 12, pp. 2149–2161, Dec. 2015. [Online]. Available: https://www.ncbi.nlm.nih.gov/pmc/articles/PMC5555767/

[45] S. Sikdar, J. P. Shah, E. Gilliams, T. Gebreab, and L. H. Gerber, "Assessment of myofascial trigger points (MTrPs): a new application of ultrasound imaging and vibration sonoelastography," *Conference proceedings: ... Annual International Conference of the IEEE Engineering in Medicine and Biology Society. IEEE Engineering in Medicine and Biology Society. Annual Conference*, vol. 2008, pp. 5585–5588, 2008.

[46] J. J. Ballyns, J. P. Shah, J. Hammond, T. Gebreab, L. H. Gerber, and S. Sikdar, "Objective sonographic measures for characterizing myofascial trigger points associated with cervical pain," *Journal of Ultrasound in Medicine: Official Journal of the American Institute of Ultrasound in Medicine*, vol. 30, no. 10, pp. 1331–1340, Oct. 2011.

[47] J.-L. Gennisson, T. Deffieux, E. Mac, G. Montaldo, M. Fink, and M. Tanter, "Viscoelastic and anisotropic mechanical properties of in vivo muscle tissue assessed by supersonic shear imaging," *Ultrasound in Medicine & Biology*, vol. 36, no. 5, pp. 789–801, May 2010.

[48] A. Windisch, A. Reitinger, H. Traxler, H. Radner, C. Neumayer, W. Feigl, and W. Firbas, "Morphology and histochemistry of myogelosis," *Clinical Anatomy (New York, N.Y.)*, vol. 12, no. 4, pp. 266–271, 1999.

[49] A. M. Alfuraih, P. O'Connor, E. Hensor, A. L. Tan, P. Emery, and R. J. Wakefield, "The effect of unit, depth, and probe load on the reliability of muscle shear wave elastography: Variables affecting reliability of SWE," *Journal of clinical ultrasound: JCU*, vol. 46, no. 2, pp. 108–115, Feb. 2018.

Curriculum Vitae

Matthew Bird currently attends George Mason University and is a candidate for his Master of Science in Bioengineering. He graduated from George Mason University with a Bachelors of Science in Bioengineering in 2016. As an undergraduate student, he was selected to participate in the Aspiring Scientists Summer Internship Program where his research focused on identifying differences in the white matter structures of the brain caused by a gene which predisposes its carriers to Alzheimers disease. He then continued his Alzheimers research as a participant in the Undergraduate Research Scholars Program. His senior design project team was awarded the George Mason University Outstanding Senior Design Award for their work in creating a noninvasive method for the diagnosis of shunt failure through the use of ultrasound. Upon graduation he immediately began studies for a Master of Science in Bioengineering at George Mason University with a focus on quantitative imaging and image analysis. While a graduate student, he presented at multiple conferences and served as a Graduate Research Assistant for two bioengineering courses.